HHS Public Access

Author manuscript

J Phys Chem B. Author manuscript; available in PMC 2021 December 10.

Published in final edited form as:

J Phys Chem B. 2020 December 10; 124(49): 11067–11071. doi:10.1021/acs.jpcb.0c05669.

Conjecture on the Design of Helical Proteins

John J. Kozak[*,a], **Harry B. Gray**[*,b]

[a]Department of Chemistry, DePaul University, Chicago IL 60604-6116.

[b]Beckman Institute, California Institute of Technology, Pasadena, CA 91125

Abstract

In an important advance in our understanding of protein folding, Wolynes and Onuchic found that the frustration ratio, T_f/T_s, for funneled energy Landscapes is $T_f/T_s \sim 1.6$. In recent work on four heme proteins, we showed that when a protein unfolds from the native state to an early unfolded state, the degree of departure is characterized by a ratio $f \sim 1.6$, where f is a measure of the elongation of n-residue segments of the polypeptide chain. Our analysis, which accounts for this apparent similarity in calculated signatures, is based on a logistic-map model of unfolding. We offer an important take home for the *de novo* protein synthesis community: in order to increase the probability of obtaining good quality crystals, nearest-neighbor repulsive interactions between adjacent residues (or sequences of residues) in the polypeptide chain must be propagated correctly.

INTRODUCTION

In 1948 Walter Kauzmann published a study on the nature of the glassy state [1]; importantly, he showed that the entropy of a liquid, which decreases rapidly on cooling towards the kinetic glass transition temperature, extrapolates to unreasonable values at lower temperatures. The temperature where the extrapolated liquid entropy is equal to the crystal entropy is called the Kauzmann temperature.

Thermodynamics, with Planck's formulation of the third law, states that the entropy of a liquid cannot be less than the entropy of a glass with the same enthalpy. This thermodynamic condition, which is in violation of the above extrapolation, is referred to as the Kauzmann paradox.

The glass-transition temperature T_g of a material characterizes the range of temperatures over which the glass transition occurs. It always is lower than the melting temperature, T_m, of the crystalline state of the material, if one exists.

Later, in the study of spin glasses, the term frustration was introduced to describe how conflicting interatomic forces lead to quite complex structures [2,3].

[*]Corresponding Author: hbgray@caltech.edu (H.B.G.); KOZAK@depaul.edu (J. J. K.).

Notes

The authors declare no competing financial interest.

Peter Wolynes and Jose Onuchic [4,5] were the first to suggest that protein folding is guided by the principle of minimal frustration, meaning that naturally evolved proteins have reduced or eliminated the deep traps that create high barriers in funneled landscapes for conversion to stable folded states. Even though nature has reduced the level of frustration, some degree remains, as documented by the presence of local minima in globally optimized energy landscapes.

A consequence of evolutionarily selected sequences is that a protein is thought to have a "globally funneled energy landscape" that is directed toward the native state. This funneled landscape allows the protein to fold to the native state through any one of a large number of pathways and intermediates, rather than being restricted to a single excursion. For a protein to be minimally frustrated, energy landscape theory shows that its folding temperature (T_f) must exceed its glass transition temperature (T_g). Onuchic and Wolynes [4,5] found that the frustration ratio, T_f/T_s, for funneled energy landscapes is $T_f/T_s \sim 1.6$.

A seminal insight on the importance of excluded volume effects on the interaction between and among proteins in solution was presented by Kauzmann in 1954 [6], later elaborated in [7]. Following earlier work by Edsall [8] and Flory [9], he noted that in the expression for the osmotic pressure of a protein as a power series in protein concentration, the second osmotic virial coefficient is directly related to the protein's excluded volume. From this insight he suggested that the polypeptide chains and amino acid side chains of proteins are folded into specific conformations that exist in the native protein. Regions included in the constitutive volumes of different portion of the molecule will fail to pack perfectly with each other. As a result, voids occur in some parts of the folded molecule, and compressed regions also may appear. The resulting conformation is made up of the net contribution of these voids and compressed regions.

The importance of excluded volume effects in the turning regions of cytochromes and globins was highlighted in our earlier work [10,11]. These effects, the consequence of repulsive forces between and among the residues of a polypeptide chain, can be gauged by considering molecular volume data for the amino acids.

Most recently, we presented molecular volume data for individual helical regions in two cytochromes and two globins [12]. If the average molecular volume is calculated for all residues in these four heme proteins, the following values are obtained:

$$\text{cyt c-b}_{562} \; \langle V \rangle = 131.77 \; \mathring{A}^3$$

$$\text{cyt c}' \; \langle V \rangle = 127.57 \; \mathring{A}^3$$

$$\text{SW-Mb} \; \langle V \rangle = 137.80 \; \mathring{A}^3$$

$$\text{h}-\text{Cygb} \ < \text{V} > \ = 135.74 \ \mathring{A}^3$$

It is remarkable that when all residues in each protein are considered, the maximum spread in average values <V> calculated for these proteins is ~ 10 $Å^3$. In fact, when we compiled a list of the percentage of each amino acid in each of the above proteins, we found that the above averages are a consequence of the dominant contribution of six residues: ALA, ASP, GLU, LEU, LYS and VAL.

The calculated averages reflect the net influence of steric interactions between and among residues in the polypeptide chain. The data show that the role of repulsive interactions in determining the native structure of proteins for which helices are the dominant structural motif is surprisingly universal. In [10] we argued that minimization of steric constraints is critical for *de novo* protein synthesis.

The above considerations on excluded volume effects naturally raise the question of whether there are other protein signatures that display such universality. In the example presented in [10], we considered first the native state of cyt c-b_{562} and, in particular, the five-residue segment, residues i-2 to i+2 centered on residue i=3.

This segment spans a distance encompassing one turn of an α-helix. The distance between the α-carbons of the terminal residues, i-2 and i+2, was calculated from crystallographic data to be R_{01to05} = 6.211 Å.

Exploring the unfolding of the native state, we then considered a fully extended configuration of residues wherein steric constraints were significantly minimized [Dummy_Incomplete] This state is represented by a planar configuration in which the triplet [i-2, i-1, i] isannexed to the triplet [i, i+1, i+2]. In this case, the distance between terminal residues, i-2 to i+2, again calculated from crystallographic data, is T(i) = 12.301 Å.

The ratio of these two distances is: *ratio* = $T(3)/R_{01to05}$ = 1.981.

In Appendix 1 of [11], we established that that this (dimensionless) ratio is exactly equal to the spatial signature $f_i = f_3$ that gives the displacement of the α-carbon of the central residue i=3 from the Fe atom (taken as the origin of the coordinate system) relative to the native state (f_i = 1) as the protein unfolds. This result is general. Given any residue i, any segment i-j to i+j, at any stage of unfolding, the calculated ratio is exactly equal to f_i.

Values of the above ratio changed when we considered the residues in all helical and turning regions in cyt c-b_{562}. Figure 1 displays the ratio (and f_i) versus residue number i in the first stage of unfolding for cyt c-b_{562}.

The all-residue, average value of this ratio (the upper horizontal line in Fig. 1) is <*ratio*> = 1.650. This average, a global signature for the protein as a whole, characterizes the (first) unfolded state in which steric constraints among residues in both helical and turning regions are minimized.

Although the value, <*ratio*> = 1.650, was calculated from data on a single iron protein, cyt c-b_{562}, we show in Table 1 of [10] (see also [11] and Table 2) that a similar result, <*ratio*> ~ 1.6, holds for cyt c', sw-Mb and h-Cygb. It is of interest to ask whether this common value is "accidental" or the consequence of an underlying principle, a matter to which we now turn.

Results and Discussion

Model of Unfolding:

Consider a representation in which, for simplicity, we adopt a system of units where the distance between terminal α-carbons in the segment i-2 to i+2 is normalized to unity, i.e., the segment i-2 to i+2 is bounded by the interval [0,1]. We construct a square with sides equal to 1. The central residue i in the segment [0,1] will be at the position ½, the midpoint of each side. We calculate the distance between the origin [0,0] and the upper-right-hand vertex [1,1] of the square using the Theorem of Pythagorus:

$$\text{distance} = \text{sqrt}\left[(1)^{\wedge}2 + (1)^{\wedge}2\right] = \text{sqrt}(2) \sim 1.414.$$

In reduced units, the distance between residues i-2 to i+2 in the native state increases by 0.414. Overall, the distance of separation between the α-carbons of residues i-2 to i+2 increases from R_{01to05} (the native state) to 1.414 R_{01to05} in the new, extended state. For cyt c-b_{562} this translates to a distance of separation between residues i-2 to i+2 of 8.782 Å. This distance is intermediate between the calculated value of R_{01to05} in the native state (6.211 Å) and the distance T(3) between terminal residues in the fully expanded, planar configuration (12.301 Å).

Relative to the distance T(3), the difference in distance [T(3) – 1.414 R_{01to05}] for residue i=3 translates into a percent difference of 28.6%. However, when *all* residues of cyt c-b_{562} are considered, the overall average percent difference is 11.9%. This more modest (all residue) percent difference suggests that studying the unfolding geometry of the intermediate state (*vide supra*) may lead to insights on the unfolding of a polypeptide chain to a fully extended state in which steric constraints are completely relaxed. This possibility will now be examined quantitatively.

The distance between the midpoint (½) on the left vertical axis of the unit square and the upper right-hand vertex can be calculated.

$$\text{distance} = \text{sqrt}\left[(1/2)^{\wedge}2 + (1)^{\wedge}2\right] = 1.118.$$

In the intermediate, expanded configuration, this is the (reduced) distance between the midpoint residue i in the segment, i-2 to i+2, and the residue i+2.

Using the diagonal (1.118) as a radius, an arc formed from the midpoint ½ intercepts the left-hand axis at a distance of 1.118 from the midpoint ½. The total distance from the origin [0,0] is then,

$$\text{Elongation in first stage} = E_1 = 0.5 + 1.118 = 1.618$$

or, more precisely, [sqrt (5) + 1] / 2 = 1.61803398875… a number known as the *Golden Ratio*. In reduced units, the segment i-2 to i+2 is bounded by the interval [0,1], so

$$ratio = 1.618/1 = 1.618.$$

(The same value of the *ratio* is obtained when reduced distances are converted to Ångstroms.)

The above procedure can be generalized. The distance from the midpoint 1/2 to the upper right-hand vertex of the rectangle generated in the previous iteration is

$$\text{distance} = \text{sqrt}\left[(1)^{\wedge}2 + (1.618)^{\wedge}2\right] = 1.902$$

Taking 1.902 as the radius of a circle with center at 1/2, the arc generated intercepts the left-hand axis at a distance of 1.902 from 1/2, a distance 0.284 greater than 1.618. Hence, the total distance from the origin [0,0] is the elongation in the second stage: $E_2 = 0.5 + 1.118 + 0.284 = 1.902$, or *ratio* = 1.902/1 = 1.902.

The two values of the *ratio*, 1.618 and 1.902, can be compared with values of the <*ratio*> given in Table 1 in [10] (*vide infra*) for two stages of unfolding in the cytochromes and globins, *viz.*, a five-residue extension that encompasses *one* turn of an α-helix and an eleven-residue segment that involves *three* turns.

A general expression for the elongation E_n (and hence the *ratio* = E_n /1) can be developed. In the first stage, as noted above,

$$E_1 = \text{sqrt}[(1 + \text{sqrt}(5))/2)^2\Big].$$

For this and subsequent stages of unfolding

$$E_n = \text{sqrt}[(n - 1) + (1 + \text{sqrt}(5))/2)^2\Big]$$

where the index $n \geq 1$. In fact, by considering fixed points other than ½, a geometrical analysis exactly similar to the one described above can be used to derive a general expression, valid for any stage of unfolding,

$$E_{n*} = \text{sqrt}[(n/4) + (1 + \text{sqrt}(5))/2)^2\Big]$$

from which values of E_n (for any n) can be recovered. Results for E_n for integer values of n ≤ 25 are displayed in Figure 2. Theoretical values of the *ratio* for each stage of unfolding considered in our study are set out in Table 1.

The gradual increase in the *global* ratio as the protein unfolds is a measure of the increase in the overall, average displacement <f> of *all* residues from the metal atom at each stage of unfolding. See Appendix 1 of [11].

Qualitatively, increases in <f> in the early stages of unfolding are more pronounced than in later stages, behavior that is confirmed quantitatively by calculating an elongation quotient

$$Q = (E_{n-1} - E_{n-2})/(E_n - E_{n-1}).$$

For n=3, Q = 1.151; for n=20, Q = 1.025.

Summarized in Table 2 are values of the <*ratio*> calculated from crystallographic data for four heme proteins, cyt c-b_{562} (106 residues), cyt c' (123 residues), sw-Mb (151 residues), and h-Cygb (188 residues). The percent difference between each calculated value of the <*ratio* >, and the theoretical value, *ratio* (= E_n/1), % = [<*ratio*> – *ratio*] / *ratio* x 100 is given in parentheses below each entry.

To assess the generality of our approach, we ask the following two questions. What are the results for a helical protein with no metal ion? And, what are the results for a helical protein with a different metal ion? To address the first question we consider Rd apo b_{562} [13], which differs from the holoprotein by seven residues and has one fewer α-helix. To address the second question, we consider the membrane protein KcsA K^+ [14]; chain C of this protein has 103 residues, three helices and a potassium ion (K^+). See Table 3.

Overall, the agreement between the theoretical *ratio* values (Table 1) and those calculated from crystallographic data for all six proteins is remarkable.

Logistic Map:

We make the formal identification, $E_n^2 \equiv Z_n$. The general expression for the elongation,

$$E_n = \mathrm{sqrt}[(n-1) + (1 + \mathrm{sqrt}(5))/2)^2$$

for the first few stages can be written as follows:

$$n = 1\ Z_1 = 0 + (1 + \mathrm{sqrt}(5))/2)^2$$

$$n = 2\ Z_2 = 1 + (1 + \mathrm{sqrt}(5))/2)^2 = Z_1 + 1$$

$$n = 3\ Z_3 = 2 + (1 + \mathrm{sqrt}(5))/2)^2 = Z_2 + 1$$

$$n = 4\ Z_4 = 3 + (1 + \mathrm{sgrt}(5))/2)^2 = Z_3 + 1$$

or, for all n ≥1,

$$Z_{n+1} = Z_n + C \text{ with } C = 1,$$

a *linear* equation. The input from one stage Z_n is used to generate the output Z_{n+1} of the next stage, an iterative process called "*feedback*." Information encoded in the n^{th} stage is transmitted to the $n+1^{th}$ stage, so that memory of a given precursor stage persists in the stage immediately following. The unfolding geometry at each stage, which is *Euclidean*, is uniquely determined.

This situation can change dramatically if the simplest *non*linear equations are studied. For example, were the linear equation to be replaced by the nonlinear (quadratic) equation,

$$Z_{n+1} = Z_n^2 + C \text{ with } C = \text{a complex number}$$

graphical representation of iterates of this equation generates the Mandelbrot set [15], self-similar patterns of amazing complexity and beauty. Here, "feedback" generates a *fractal* geometry rather than the Euclidean geometry of the linear equation. If the linear equation is replaced by May's logistic map [16]

$$Z_{n+1} = kZ_n(1 - Z_n) \text{ with } k = \text{a constant}$$

iterates of this nonlinear equation depend sensitively on the value of the constant k.

Edward Lorenz called this sensitive dependence on initial conditions (values of the constant k), in which a small change in one state of a deterministic nonlinear system can result in large differences in a later state, the "butterfly effect" [17].

The patterns generated are *chaotic*.

As noted above, successive stages in the *unfolding* of a protein generated by the linear equation, $Z_{n+1} = Z_n + C$, are correlated, with the *memory* of steric constraints in the n^{th} stage of unfolding incorporated in the $n+1^{th}$ stage.

Correlations arising from the minimization of repulsive forces among residues are propagated from one extended state to the next. In the reciprocal problem of protein *folding*, reverse iteration of the (deterministic) *linear* equation from state n +1 to state n will generate a specific conformation that is globally minimized with respect to excluded volume effects.

Each successive conformation will be described by *Euclidean* geometry; and the final crystal structure of the protein is uniquely determined.

If May's logistic equation is used, even small fluctuations in ambient conditions will influence the iterative process. Each initial condition will result in a different conformation, disfavoring crystallization of the protein. It is apparent that folding the Parkinson's protein α-synuclein [18], which has not been (cannot be?) crystallized, is not guided by a deterministic *linear* equation ($Z_{n+1} = Z_n + C$).

Conclusions

We begin by noting that the geometric construction described above, which leads to the Golden Ratio, was the one used by medieval craftsmen in building the Gothic Cathedral of Chartres in the 12th century. The Golden Ratio also emerges in analyzing the sequence, 0, 1, 1, 2, 3, 5, 8, 13, 21, 34, etc., discovered by Fibonacci in 1202. As was shown first by Simon in 1564 and rediscovered by Kepler in 1608, if a Fibonacci number is divided by its immediate predecessor, the sequence of values calculated converges rapidly to the Golden Ratio. Among the many examples of the Golden Ratio in Nature are leaf divergence in plants as well as spirals in sunflowers and Nautilus shells.

We have argued [10] that excluded volume effects (resulting in steric restrictions) should be taken into account in designing *de novo* protein syntheses [19–22].

Here, we have shown that when a protein begins to unfold it opts for a state (or states) in which repulsive forces are relaxed. When we explore the simplest mathematical models (or, to use a metaphor from computer science, "operating systems") for protein denaturation, *viz.*, the *linear* equation [$Z_{n+1} = Z_n + C$] *versus* two *non*linear equations, the Mandelbrot set [$Z_{n+1} = Z_n^2 + C$] and May's logistic map [$Z_{n+1} = k Z_n (1 - Z_n)$], we find that, already in studying an *intermediate* stage of unfolding in which steric constraints are only partially relaxed, the Golden Ratio (embedded in the *linear* equation) emerges as a design principle driving denaturation.

The same design principle is found in phyllotaxis. It maximizes the space for each leaf on a stem (an excluded volume effect), while helping to optimize exposure to the sun. In seashells, like the Chambered Nautilus, the pattern allows the organism to grow without changing shape. In the early stages of unfolding of a protein, it enables (quasi) persistence of the native structure. It is astonishing that the design principle used to construct Chartres (and earlier, the Great Pyramid of Giaz and the Parthenon) is the same as that governing the unfolding of proteins.

In summary, we have shown that there is a correspondence between *frustration* in the energy landscape model of *folding* and *excluded volume effects* in our angular landscape model of *unfolding*. It is our view that the protein folding field owes much to the seminal work of Walter Kauzmann: his 1948 article on glasses [1] led eventually to the principle of minimal frustration introduced by Wolynes and Onuchic [4,5]; and his 1959 article on denaturation [6] led to our work on excluded volume effects on protein stability [10–11].

ACKNOWLEDGEMENTS

The authors thank R. A. Garza-López for helpful discussions. Work at Caltech was supported by the NIH (DK019038) and the Arnold and Mabel Beckman Foundation.

REFERENCES

1. Kauzmann W The Nature of the Glassy State and the Behavior of Liquids at Low Temperatures. Chem. Rev 1948, 43, 219–256.
2. Binder K; Young AP (1986) Spin glasses: Experimental facts, theoretical concepts, and open questions. Rev. Mod. Phys. 1986, 58, 801–976.
3. Mydosh JA Spin glasses: redux: an updated experimental/materials survey. Rev Mod Phys 2015, 78, 1–25.
4. Bryngelson JD; Onuchic JN; Socci ND; Wolynes PG Funnels, pathways, and the energy landscape of protein folding: a synthesis. Proteins 1995, 21, 167–95. [PubMed: 7784423]
5. Leopold PE; Montal M; Onuchic JN Protein folding funnels: a kinetic approach to the sequence-structure relationship. Proc. Natl. Acad. Sci. USA 1992, 89, 8721–8725. [PubMed: 1528885]
6. Kauzmann W Some factors in the interpretation of protein denaturation. Adv. Protein. Chem 1959, 14, 1–63. [PubMed: 14404936]
7. Kozak JJ; Knight WS; Kauzmann W Solute-solute Interactions in Aqueous Solution. J. Chem. Phys 1968, 48, 675–690.
8. Edsall JT The Proteins (Neurath H; Bailey K, eds), Vol. I, Part B, Chapter 7, Academic Press, New York, 1953.
9. Flory PJ Principles of Polymer Chemistry, Cornell Univ. Press, Ithaca, New York, 1953.
10. Kozak JJ; Gray HB Stereochemistry of residues in turning regions of helical proteins. J. Biol. Inorg. Chem 2019, 24, 879–888. [PubMed: 31511993]
11. Kozak JJ; Gray HB; Garza-Lopez RA Funneled angle landscapes for helical proteins. J. Inorg. Biochem 2020, 208, 111091(1–13). [PubMed: 32497828]
12. Kozak JJ; Gray HB; Garza-Lopez RA Structural stability of the SARS main protease: Can metal ions affect function? J. Inorg. Biochem 2020.
13. Feng H; Zhou Z; Bai Y A protein folding pathway with multiple folding intermediates at atomic resolution. Proc. Natl. Acad. Sci. USA 2005, 102, 5026–5031. [PubMed: 15793003]
14. Doyle DA; Cabral J; Pfuetzner RA; Kuo A; Gulbis JM; Cohen SL; Chait BT; MacKinnon R (1998) The Structure of the Potassium Channel: Molecular Basis of K+ Conduction and Selectivity. Science 1998, 280, 69–77.
15. Mandelbrot B The Fractal Geometry of Nature. W.H. Freeman and Company, 1982.
16. May RM Simple mathematical models with very complicated Dynamics. Nature 1976, 560, 459–467
17. Lorenz E The Essence of Chaos, p. 14, University of Washington Press, 1993.
18. Lee JC; Lai BT; Kozak JJ; Gray HB; Winkler JR α-Synuclein Tertiary Contact Dynamics. J. Phys. Chem 2007, 111, 2107–2112.
19. Korendovych IV; DeGrado WF De novo protein design, a retrospective. Quart. Rev. Biophysics 2020, 53, e3, 1–33.
20. Brunette TJ; Parmeggiani F; Huang PS; Bhabha G; Ekiert DC; Tsutakawa SE; Hura GK; Tainer JA; Baker D Exploring the repeat protein universe through computational protein design. Nature 2015, 528, 58–584.
21. Calhoun JR; Kono H; Lahr S; Wang W; DeGrado WF; Saven JG Computational design and characterization of a monomeric helical dinuclear metalloprotein. J. Mol. Biol 2003, 334, 1101–1115. [PubMed: 14643669]
22. Plegaria JS; Pecoraro VL (2016) *De novo* design of metalloproteins and metalloenzymes in a three-helix bundle. Methods Mol. Biol. 2016, 1414, 187–196.

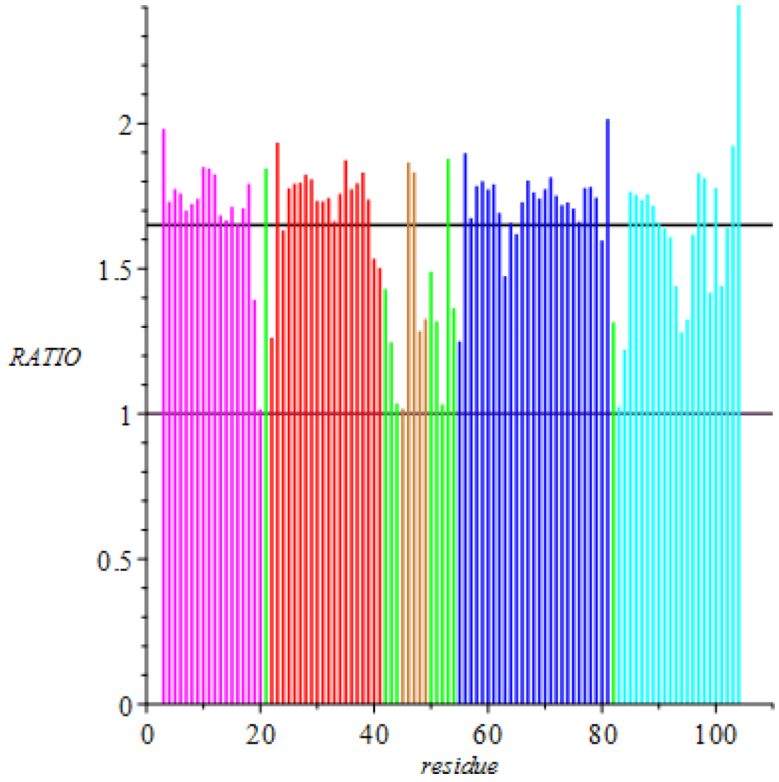

Figure 1.
The *ratio* T(i) / R(i-2) to R(i+2) vs residue number for cyt c-b_{562}.

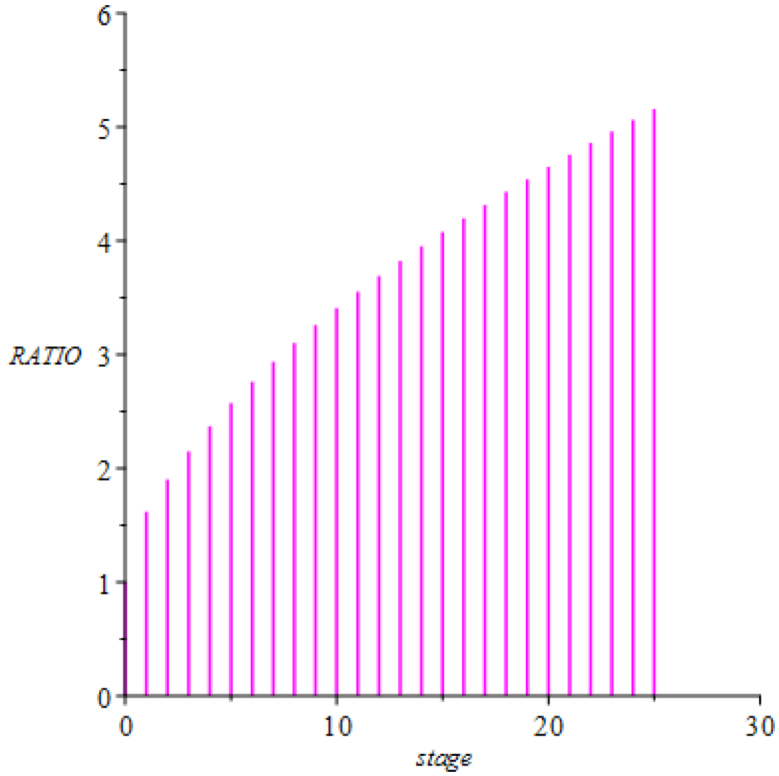

Figure 2.
The *ratio* (= E_n /1) *versus* unfolding stage (n).

Table 1.

Theoretical *ratio* values for each stage of unfolding.

Segment ***ratio***	**Number of Residues**	**Turns of an α-helix**		**Index n**
R(i−1) to R(i+1)	3	0		
R(i−2) to R(i+2)	5	1	1	1.618
R(i−3) to R(i+3)	7	1	1*	1.694
R(i−4) to R(i+4)	9	2	2*	1.766
R(i−5) to R(i+5)	11	3	2	1.902
R(i−6) to R(i+6)	13	3	3	2.148
R(i−7) to R(i+7)	15	4	4	2.370

Table 2.

Unfolding the polypeptide chain. Values of *<ratio>* for each stage.

<ratio>	**cyt c-b_{562}**	**cyt c'**	**sw-Mb**	**h-Cygb**
T(i)/ R(i−1) to R(i+1)	1.0	1.0	1.0	1.0
T(i)/ R(i−2) to R(i+2)	1.650	1.604	1.674	1.601
	(2.0%)	(−0.9%)	(3.5%)	(−1.1%)
T(i)/ R(i−3) to R(i+3)	1.655	1.637	1.696	1.676
	(2.3%)	(1.2%)	(4.8%)	(3.6%)
T(i)/ R(i−4) to R(i+4)	1.841	1.782	1.862	1.832
	(4.2 %)	(0.9%)	(5.4%)	(3.7%)
T(i)/ R(i−5) to R(i+5)	1.968	1.915	1.984	1.984
	(2.9%)	(0.7%)	(4.3%)	(4.3%)
T(i)/ R(i−6) to R(i+6)	2.153	2.059	2.121	2.131
	(0.2%)	(−4.2%)	(−1.3%)	(−0.8%)
T(i)/ R(i−7) to R(i+7)	2.290	2.228	2.306	2.319
	(−0.3%)	(−5.9%)	(−2.7%)	(−2.2%)

Table 3.

Unfolding a polypeptide chain. Values of *<ratio>* for each stage.

<ratio>	Rd apo b_{562}	KcsA K^+ (chain C)
T(i)/ R(i−1) to R(i+1)	1.0	1.0
T(i)/ R(i−2) to R(i+2)	1.625	1.648
	(0.4%)	(1.9%)
T(i)/ R(i−3) to R(i+3)	1.638	1.674
	(1.2%)	(3.5%)
T(i)/ R(i−4) to R(i+4)	1.787	1.851
	(1.2%)	(4.8%)
T(i)/ R(i−5) to R(i+5)	1.892	1.968
	(−0.5%)	(3.5%)
T(i)/ R(i−6) to R(i+6)	2.046	2.148
	(−4.8%)	(0.0%)
T(i)/ R(i−7) to R(i+7)	2.182	2.32
	(1.5%)	(−1.9%)